Journal of Statistical Physics, Vol. 70, Nos. 3/4, 1993

A Maximum Entropy Mean Field Method for Driven Diffusive Systems

N. C. Pesheva,[1] Yitzhak Shnidman,[2] and R. K. P. Zia[3]

Received August 30, 1991; final August 6; 1992

We introduce a method of generating systematic mean field (MF) approximations for the nonequilibrium steady state of ferromagnetic Ising driven diffusive systems (DDS), based on the maximum entropy principle due to Jaynes. In the phase coexistence region, MF approximations to the master equation do not provide a closed system of equations in the MF variables. This can be traced to the conservation of the order parameter by the stochastic dynamics. Our maximum entropy mean field (MEMF) approximation method is applicable to high temperatures as well to the low-temperature phase coexistence region. It is based on a derivation of a generalized variational free energy from the maximum entropy principle, with the MF evolution equations playing the role of constraints. In the phase coexistence region this free energy is nonconvex and is interpreted by means of a Maxwell construction. We use a pair-level variant of the MEMF approximation to calculate quantities of interest for the ferromagnetic Ising DDS on a square lattice. Results of calculations with several different choices of transition rates satisfying local detailed balance are discussed and compared with those obtained by other methods.

KEY WORDS: Kinetic lattice models; nonequilibrium steady state; maximum entropy principle; mean field methods.

1. INTRODUCTION

The statistical mechanics of cooperative systems in thermal equilibrium with a heat reservoir is fairly well understood. By comparison, much less is known about such systems when driven out of equilibrium by some external

[1] Institute of Mechanics and Biomechanics, Bulgarian Academy of Sciences, Acad. G. Bonchev St 4, 1113 Sofia, Bulgaria.

[2] Research Laboratories, RTSS Division, Eastman Kodak Company, Rochester, New York 14650-2216.

[3] Department of Physics and Center for Stochastic Processes in Science and Engineering, Virginia Polytechnic Institute and State University, Blacksburg, Virginia 24061.

822/70/3-4-15

force. Historically, simple lattice models were instrumental in gaining our current understanding of equilibrium cooperative phenomena. One may hope that a similar approach will be helpful for the nonequilibrium case as well. The Ising driven diffusive system (DDS),[1,2] which is studied here, is one of the simplest lattice models exhibiting nonequilibrium phase transitions. It is a kinetic Ising[3–5] (or, equivalently, a lattice-gas) model defined on a lattice with periodic boundary conditions. Its time evolution is governed by stochastic pair exchange transition rates that are biased in a certain direction by a driving field **E**. For $\mathbf{E}=0$, the usual equilibrium Ising behavior is recovered at long times, but finite fields drive the system into a nonequilibrium steady state (NESS). A detailed definition of the Ising DDS is given in Section 2, where results of simulations and other studies of this model are also described. These results indicate that, while phase separation still occurs as the reservoir temperature T_R is lowered, the underlying statistics at NESS seems to be qualitatively different from the equilibrium case. It is the statistics of the Ising DDS at NESS that is the subject of this work. Specifically, we propose here a new method of generating a hierarchy of successive mean field (MF) approximations to it that is based on the maximum entropy principle (MEP).[6–10]

The master equation is a system of 2^N-1 independent *linear* equations for the joint probability distribution of the spin configurations of N sites. In Section 3 we show how, under well-defined MF assumptions, a hierarchy of approximations is derived from the master equation. This leads to a set of evolution equations for the MF variables that conserve the local order parameter m and are identical to the equations of Dickman's dynamical MF theory.[11] At a NESS specified by fixed T_R and **E**, they are reduced to a system of $n-1$ independent *nonlinear* algebraic equations for n independent MF variables corresponding to a given level of approximation. Since m obeys a conservation law, its evolution does not contribute a nontrivial algebraic equation at NESS. In the disordered phase, $m=0$, and hence the system of equations is closed and can always be solved numerically. In the phase coexistence region, however, m is an unknown variable, which depends on T_R and **E**, so that the system of equations is incomplete and cannot be solved.

In Section 4, which is the centerpiece of this work, we overcome this difficulty by using the MEP to generate a complete system of MF equations for DDS at NESS, for all T_R and **E**. Bowers and McKerrel[12] have shown that, for nonequilibrium systems in thermal contact with a heat reservoir, the MEP is equivalent to a minimum principle for a generalized Helmholtz free energy. We derive here a MF approximation for the generalized Helmholtz free energy of the DDS system. For specified T_R and **E**, the later is a function of the n independent MF variables on a given level

of approximation. These variables play the role of variational parameters for the MF approximation to the generalized Helmholtz free energy. At a NESS, the MF evolution equations (at the same level of approximation) translate into $n-1$ nonlinear constraints for these variables. In this way, $\mathbf{E}$ is taken into account. The generalized Helmholtz free energy is convex in the disordered phase, with a unique global minimuim identical with the $m=0$ steady-state solution of the MF evolution equations. However, it becomes nonconvex in the phase coexistence regime and the relevant information for this region is obtained by means of a Maxwell construction.

To test our MF method, in Section 5 we apply it to the ferromagnetic Ising DDS on the square lattice with zero total magnetization. We use a pair-level variant of our MF approximation to calculate various physical quantities of interest as T_R and $\mathbf{E}$ are varied. Results are shown to be dependent on different choices of transition rates satisfying local detailed balance. These results are compared with those obtained by other methods, such as Dickman's dynamic MF theory, Kikuchi's cluster variation approximation at equilibrium, and Monte Carlo simulations. We conclude in Section 6 with a general discussion of the strengths and weaknesses of the maximum entropy MF method for DDS that has been introduced in this paper.

2. THE MODEL AND SOME KNOWN RESULTS

The Ising DDS was originally introduced by Katz *et al.*[1,2] in a stochastic lattice-gas form. A more careful definition of the lattice-gas version on the square lattice can be found in Krug *et al.*[13] We reproduce it below, recast in Ising spin language. Consider a system of Ising spins σ_i occupying the N sites i of a square lattice Λ with periodic boundary conditions. Assume the usual ferromagnetic ($J>0$) or antiferromagnetic ($J<0$) interactions between nearest-neighbor ($\langle ij\rangle$) spins σ_i and σ_j, given by the Ising Hamiltonian

$$H = -J \sum_{\langle ij\rangle} \sigma_i \sigma_j \tag{2.1}$$

where $\sigma_i = \pm 1$.

Let this system be in thermal contact with a heat reservoir at temperature T_R. Static properties of the Ising model (2.1) *at equilibrium* with a thermostat are well known. Its time evolution and transport properties on the mesoscopic scale can be modeled by different types of stochastic dynamics. In this approach the time evolution of the probability $\rho_t(\{\sigma\})$ of finding a spin configuration $\{\sigma\}$ at time t is assumed to be modeled by a

stationary Markov chain. It is completely determined by specifying the transition rates in the corresponding master equation. The form of the latter for the Ising DDS is as follows:

$$\frac{d\rho_t(\{\sigma\})}{dt} = \sum_{\langle ij\rangle} [\phi_E(i, j, \{\sigma\}^{\langle ij\rangle})\, \rho_t(\{\sigma\}^{\langle ij\rangle}) - \phi_E(i, j, \{\sigma\})\, \rho_t(\{\sigma\})] \tag{2.2}$$

Here $\{\sigma\}^{\langle ij\rangle}$ denotes a configuration $\{\sigma\}$ with the spins at nearest-neighbor sites $\langle ij\rangle$ interchanged, $\phi_E(i, j, \{\sigma\})$ are the transition rates for pair exchange of spins at $\langle ij\rangle$ from configuration $\{\sigma\}$, and E is the driving field strength biasing pair exchanges along a certain direction. For simplicity, we assume that $\mathbf{E}$ is along one of the unit lattice vectors $\hat{e}_i$, $i = 1, 2$, say $\mathbf{E} = E\hat{e}_1$. The transition rates are then defined to be

$$\phi_E(i, j, \{\sigma\}) = \begin{cases} \Gamma_{\|}\phi(\{\Delta H^{\langle ij\rangle} + E(i-j)(\sigma_i - \sigma_j)/2\}/k_B T_R)(1-\sigma_i\sigma_j)/2, & i-j = \pm\hat{e}_1 \\ \Gamma_{\perp}\phi(\Delta H^{\langle ij\rangle}/k_B T_R)(1-\sigma_i\sigma_j)/2, & i-j = \pm\hat{e}_2 \end{cases} \tag{2.3}$$

Here $\Gamma_{\|}$ and $\Gamma_{\perp}$ represent the rates for attempting exchanges of pairs parallel or perpendicular to $\mathbf{E}$, respectively. The factor $(1-\sigma_i\sigma_j)/2$ ensures that only a pair of opposite spins are exchanged. $\Delta H^{\langle ij\rangle}$ is defined as the energy gain of a configuration following a pair exchange,

$$\Delta H^{\langle ij\rangle} = H(\{\sigma\}) - H(\{\sigma\}^{\langle ij\rangle}) \tag{2.4}$$

Note that it depends only on the *local* cluster configuration of $\langle ij\rangle$ and its nearest neighbors

$$\Delta H^{\langle ij\rangle} = 2J\left(\sigma_i \sum_{\langle ik\rangle} \sigma_k + \sigma_j \sum_{\langle jl\rangle} \sigma_l - 2\sigma_i\sigma_j\right) \tag{2.5}$$

The pair exchange dynamics as defined by (2.2)–(2.3) is *spin conserving*, since the global spin operator $M = \sum_i \sigma_i$ remains constant in time. The choice of the rate function $\phi(\lambda)$ is arbitrary, as long as it satisfies the detailed balance condition

$$\phi(\lambda) = e^{-\lambda}\phi(-\lambda) \tag{2.6}$$

Equations (2.1)–(2.5) with different choices of the ratio $\Gamma_{\|}/\Gamma_{\perp}$ and with a particular form of $\phi(\lambda)$ obeying (2.6) define different variants of the Ising DDS. The constraint (2.6) ensures that, for $\mathbf{E} = 0$ and $\Gamma_{\|}, \Gamma_{\perp} > 0$,

$$\lim_{t\to\infty} \rho_t(\{\sigma\}); M) = Z^{-1} \exp(-H/k_B T_R)\, \delta\left(\sum_i \sigma_i - M\right) \tag{2.7}$$

where

$$Z = \sum_{\{\sigma\}} \exp(-H/k_B T_R)\, \delta\left(\sum_i \sigma_i - M\right) \tag{2.8}$$

The steady-state probability distribution defined by (2.7)–(2.8) corresponds to the canonical one for an Ising model (2.1) with fixed $M = \sum_i \sigma_i$ at equilibrium with a heat reservoir at temperature T_R. Note that it is *independent* of the particular choice of $\phi(\lambda)$ and $\Gamma_{||}/\Gamma_{\perp}$. The discussion in this paper is confined to Ising systems (2.1)–(2.6) with $J > 0$, $M = 0$, and from now on the term DDS is used restrictively for this case, unless explicitly stated otherwise. At $\mathbf{E} = 0$ and $\Gamma_{||}/\Gamma_{\perp} = 1$, DDS reduces to the well-known kinetic Ising model with spin-conserving Kawasaki pair exchange dynamics. On the square lattice, its equilibrium steady state undergoes phase separation when T_R is lowered below a critical temperature $k_B T_C = 2.269$ J. At $T_R > T_c$ the system is found in a single homogeneous disordered phase with the local order parameter being $\langle \sigma_i \rangle = 0$ for any i on the lattice. At $T_R < T_c$ there are two coexisting ordered phases. Except for a flat interface region oriented along one of the main lattice directions and of characteristic width comparable to the correlation length, the two phases are homogeneous, with $\langle \sigma_i \rangle = \pm m(T_R)$, where the two signs correspond to i being in either of the two phases. Moreover, the values of $\langle \sigma_i \rangle$ in the ordered phases are identical to these of the equilibrium Ising model (2.1) *without* the constraint $\sum_i \sigma_i = 0$.

The role of $\mathbf{E}$ in (2.2)–(2.3) is fashioned after a hypothetical constant electric field interacting with the Ising as though they were charges. This constant electric field *cannot* arise from a gradient of an electrostatic potential, due to the assumed periodic boundary conditions. The latter play an important role, since, in their absence, a concentration gradient will build up, leading to an equilibrium state, similar to that of gas particles confined in a box and placed in a gravitational field. Instead, we seek a nonequilibrium steady state with homogeneous phases and nonzero total current.

The $J > 0$, $M = 0$ version of the Ising DDS has recently been the subject of intensive studies by means of Monte Carlo simulations, analytic solutions to the master equation in the limits $\Gamma_{||}/\Gamma_{\perp} \to \infty$ and $E \to \infty$, and field-theoretic methods. The following picture, which is still incomplete, energes from these cumulative efforts. Following an initial relaxation time, the $\mathbf{E} \neq 0$ DDS typically attains a nonequilibrium steady state characterized by stationary current and probability distribution. The latter, however, depends not only on T_R and $\mathbf{E}$, but also on the particular choice of $\phi(\lambda)$ and $\Gamma_{||}/\Gamma_{\perp}$. The most common choices of the rate functions $\phi(\lambda)$ obeying (2.6) and the names by which they are referred to in this paper are

Table I. Transition Rates

Metropolis rates	$\phi(\lambda)=\begin{cases}\exp(-\lambda), & \lambda>0\\ 1, & \lambda\leqslant 0\end{cases}$
Kawasaki rates	$\phi(\lambda)=2/[1+\exp(\lambda)]$
Van Beijeren–Schulman rates	$\phi(\lambda)=\exp(-\lambda/2)$

$$\lambda=(\Delta H\pm\varepsilon E)/T_R, \qquad \varepsilon=0,\ \pm 1$$

listed in Table I. Most of the Monte Carlo work on the Ising DDS has been performed on the square lattice using Metropolis rate functions and $\Gamma_{||}/\Gamma_{\perp}=1$.[1,2,13–15] Results indicate that phase separation into two homogeneous ordered phases persists for all values of E, with local order parameters given now by $\langle\sigma_i\rangle=\pm m(T_R, E)$. However, a steady-state current $\mathbf{J}(T_R, E)\,\|\,\mathbf{E}$ is generated when $\mathbf{E}\neq 0$, the interface becomes oriented parallel to $\mathbf{E}$, and local anisotropy develops with respect to directions parallel and perpendicular to $\mathbf{E}$, as manifested in distinct pair correlations in those directions. The local order parameters $\pm m(T_R, E)$ vanish on a line of critical points $T_c(E)$, the latter being a monotonically increasing function of E that saturates at $T_c(E\to\infty)\approx 1.4T_c(E=0)$. The steady-state current $\mathbf{J}$ has a discontinuity in its slope at $T_c(E)$. Renormalization group calculations[16,17] predict a mean field value for the critical exponent β from an ε-expansion to all orders in $\varepsilon=5-d$. Initial finite-size scaling of square lattice simulations with Metropolis rates[15,18,19] indicated β intermediate between mean field and the equilibrium Ising one, hinting at a separate universality class at large E. However, a subsequent study by Leung[20] pointed to flaws in these works and proposed a new form of finite-size scaling appropriate for the DDS at nonvanishing $\mathbf{E}$, which results in $\beta=1/2$.

Previous attempts to develop mean field approximation methods included a mean field approximation to the master equation in the limit $E\to\infty$, $\Gamma_{||}/\Gamma_{\perp}\to\infty$. Solutions of the MF master equation in the limit $E\to\infty$, $\Gamma_{||}/\Gamma_{\perp}\to\infty$ yield[21,13] T_c that varies significantly for the three different choices of the rate function ϕ in Table I. Monte Carlo simulations with explicitly varying $\Gamma_{||}/\Gamma_{\perp}$ also show[18] nontrivial dependence of $T_c(E)$ and other system properties on this ratio. A different MF approximation to the master equation of the DDS has been derived by Dickman[11] based on a dynamic cluster variation method. His approach results in a system of algebraic equations in the cluster probabilities, which are asumed to be translationaly invariant throughout the entire system. However, it is valid

only in the disordered phase, since this system of equations is not closed (there are more independent variables than equations) in the coexistence region of the ferromagnetic DDS. This is due to the conservation of the order parameter by the stochastic equations of motion in the ferromagnetic DDS. Nevertheless, Dickman proceeded to estimate the field-dependent critical temperatures by investigating the limits of stability of the zero-magnetization solution under the imposition of small magnetization gradients. This approach was subsequently applied[22] to the antiferromagnetic DDS, where the system of equations is closed for any choice to T_R and **E**, since the order parameter is not conserved in this case. Recently, Garrido *et al.*[23] have alsol tried to circumvent the failure of closure of the dynamic MF equations for the ferromagnetic DDS by explicit consideration of the MF evolution equations at a sharply defined interface.

For a detailed survey of various studies of the DDS model the reader is referred to the recent comprehensive review article by Schmittmann.[24]

3. MEAN FIELD EVOLUTION EQUATIONS

An exact analytical solution of (2.2) is not within reach. A systematic approach of generating approximate solutions to (2.2) is provided by a generalization of the cluster variation method. This technique was originally developed by Kikuchi[25] as a way to generate systematic approximations for the free energy of Ising systems *at equilibrium*. Here we use a reformulation of this approximation due to Morita.[26] In this method, the joint probability distribution for the *whole* system is expressed through *reduced* probability distributions for finite clusters, by neglecting higher-order correlations.

Consider the n-point reduced probability distribution functions $\rho_t^{(n)}$ of finding configurations $\{\sigma\}^{(n)} = \{\sigma_{i_1},...,\sigma_{i_n}\}$ at time t on a cluster of points $i_1,...,i_n$ that are a subgraph of a square lattice containing N points. These are obtained from the joint probability distribution $\rho_t \equiv \rho_t^{(N)}$ for the entire lattice as follows:

$$\rho_t^{(n)}(\sigma_1,...,\sigma_{i_n}) = \sum_{\{\sigma\}^{(N)} - \{\sigma\}^{(n)}} \rho_t^{(n)}(\sigma_1,...,\sigma_{i_n}) \tag{3.1}$$

The summation is over all configurations in the part of the phase space which is complementary to the phase space of the cluster $i_1,...,i_n$. Following Morita, let us recursively define a hierarchy of n-spin functions $\eta_t^{(n)}$ that are a measure of the correlation between the n spins:

$$\eta_t^{(2)}(\sigma_i, \sigma_j) = \frac{\rho_t^{(2)}(\sigma_i, \sigma_j)}{\rho_t^{(1)}(\sigma_i)\, \rho_t^{(1)}(\sigma_j)} \tag{3.2}$$

$$\vdots$$

$$\eta_t^{(n)}(\sigma_{i_1},\ldots,\sigma_{i_n}) = \rho_t^{(n)}(\sigma_{i_1},\ldots,\sigma_{i_n}) \times \left[\prod_{k=1}^{n} \rho_t^{(1)}(\sigma_{i_k}) \prod_{\{k_1,k_2\}} \eta_t^{(2)}(\sigma_{i_{k_1}}, \sigma_{i_{k_2}}) \cdots \times \prod_{\{k_1,k_2,\ldots,k_{n-1}\}} \eta_t^{(n-1)}(\sigma_{i_{k_1}}, \sigma_{i_{k_2}},\ldots,\sigma_{i_{k_{n-1}}}) \right]^{-1} \tag{3.3}$$

Here the products are over partitions of the cluster into singlets, pairs, triplets, etc., in a way that that avoids overdetermination of subcluster probabilities. The possible partitions depend on the topology of the cluster. As the simplest example, for the elementary triangle with vertices (1, 2, 3) on the triangular lattice, $\eta_t^{(3)}(\sigma_1, \sigma_2, \sigma_3)$ is given by $\rho_t^{(3)}(\sigma_1, \sigma_2, \sigma_3)$ divided by either

$$\eta_t^{(2)}(\sigma_1, \sigma_2)\, \eta_t^{(2)}(\sigma_1, \sigma_3) \prod_{i=1}^{3} \rho_t^{(1)}(\sigma_i)$$

or by the other two permutations of this expression, but not by

$$\eta_t^{(2)}(\sigma_t, \sigma_2)\, \eta_t^{(2)}(\sigma_1, \sigma_3)\, \eta_t^{(2)}(\sigma_2, \sigma_3) \prod_{i=1}^{3} \rho_t^{(1)}(\sigma_i)$$

The joint probability distribution for the entire system is then

$$\rho_t^{(N)}(\sigma_1,\ldots,\sigma_{i_n}) = \prod_{k=1}^{n} \rho_t^{(1)}(\sigma_{i_k}) \prod_{\{k_1,k_2\}} \eta_t^{(2)}(\sigma_{i_{k_1}}, \sigma_{i_{k_2}}) \cdots \eta_t^{(N)}(\sigma_{i_1},\ldots,\sigma_{i_N}) \tag{3.4}$$

On a specified level of approximation for the nonequilibrium steady-state distribution, let us consider explicitly the correlations in a given basic (connected) cluster consisting of n lattice sites and of all its subclusters (preserved clusters in Morita's terminology). Henceforth, we will drop the subscript t when writing probabilities and correlations at NESS, since they are stationary in time. We neglect the correlations in bigger clusters and between clusters that do not intersect. This is achieved by setting, for all clusters in which the correlations are neglected,

$$\eta^{(k)}(\sigma_{i_1},\ldots,\sigma_{i_k}) = 1 \tag{3.5}$$

Thus, e.g., (3.5) holds for all $k > n$. The reduced probability distributions for bigger clusters and clusters that do not intersect are found from

(3.1)–(3.5) in terms of $\rho^{(1)}, \rho^{(2)},..., \rho^{(n)}$. For simplicity, we also make the assumption of system homogeneity at the steady state. Thus we have

$$\rho^{(k)}(\sigma_{i_1},..., \sigma_{i_k}) = \rho^{(k)}(\sigma_1,..., \sigma_k) \tag{3.6}$$

for all clusters of the same size and shape. This assumption is violated at the interface between the two coexisting phases at low temperatures, whose contribution to the free energy is negligible in the infinite-system limit, relative to the bulk contribution.

From the master equation (2.2) one can derive a hierarchy of equations for the macroscopic variables (average values of spins and products of spins), which are usually referred to as rate equations. A systematic method for deriving these equations was developed by van Kampen[27] in the form of a power series expansion in a parameter related to the size of the system. On the pair level of approximation van Baal[28] has suggested such a coarse-graining procedure for both the Kawasaki and Glauber kinetic Ising models. The resulting equations are the same as those obtained in ref. 29 based on heuristic arguments. A similar systematic coarse graining of the master equation at the pair level of approximation for DDS at NESS is the subject of another paper.[30] Here the second, more heuristic approach is adopted. In this approach the equations are derived by considering explicitly all the configurations $\{\sigma\}_{cl}$ on a certain small cluster, their respective probabilities of occurring $\rho(\{\sigma\}_{cl})$, and the transition rates $\phi(\Delta H)$ for performing exchange from or to this configuration. The general form of a such an equation is

$$\frac{d\rho^{(k)}}{dt} = G^{(k)}(\rho^{(1)}, \rho^{(2)},..., \rho^{(n)}) \tag{3.7}$$

$$= \sum_{\{\sigma\}_{cl}} \Delta\rho^{(k)}\, \phi(\Delta H)\, \rho(\{\sigma\}_{cl}), \qquad k = 1, 2,..., n \tag{3.8}$$

where $\Delta\rho^{(k)}$ is the corresponding change in $\rho^{(k)}$ when exchange is performed, and $\rho(\{\sigma\}_{cl})$ is expressed through $\rho^{(1)}, \rho^{(2)},..., \rho^{(n)}$. The left-hand side of Eq. (3.7) is identicaly zero at NESS.

At the pair level of approximation the system is described in terms of the single-site and nearest-neighbor pair probability distributions $\rho^{(1)}(\sigma_i)$ and $\rho^{(2)}(\sigma_i, \sigma_j)$, respectively, i.e., one assumes

$$\eta^{(k)}(\sigma_{i_1},..., \sigma_{i_k}) = 1 \qquad \text{for} \quad k > 2 \tag{3.9}$$

and also

$$\eta^{(2)}(\sigma_i, \sigma_j) = 1 \qquad \text{for} \quad |i - j| > 1 \tag{3.10}$$

In equilibrium, the homogeneity assumption is expressed by

$$\rho^{(1)}(\sigma_i) = \rho^{(1)}(\sigma) \qquad \text{for all} \quad i \in \Lambda \tag{3.11}$$

$$\rho^{(2)}(\sigma_i, \sigma_j) = \rho^{(2)}(\sigma_1, \sigma_2) \qquad \text{for all} \quad i \in \Lambda \text{ and } j = i + \hat{e}_{1,2} \tag{3.12}$$

However, the presence of an electric field along $\hat{e}_1$ will certainly induce some anisotropy. To account for this, we have to allow different probability distributions for bonds along the field and perpendicular to it, i.e.,

$$\rho^{(2)}(\sigma_i, \sigma_{i+\hat{e}_1}) = \rho_1^{(2)}(\sigma_1, \sigma_{1+\hat{e}_1}), \qquad i \in \Lambda \tag{3.13}$$

$$\rho^{(2)}(\sigma_i, \sigma_{i+\hat{e}_2}) = \rho_2^{(2)}(\sigma_1, \sigma_{1+\hat{e}_2}), \qquad i \in \Lambda \tag{3.14}$$

as shown in Fig. 1.

Thus, on the pair level of approximation at NESS, the system is described in terms of the eight variables

$$\rho^{(1)}(+1) = x, \qquad \rho^{(1)}(-1) = y \tag{3.15}$$

$$\left.\begin{aligned} &\rho_i^{(2)}(+1, +1) = z_i \\ &\rho_i^{(2)}(+1, -1) = \rho_i^{(2)}(-1, +1) = b_i \\ &\rho_i^{(2)}(-1, -1) = w_i \end{aligned}\right\}, \qquad i = 1, 2 \tag{3.16}$$

These include the probability of a single site to have spin up, x, or down, y; the probability for two nearest-neighbor sites to have both spins up, z_i; to have both spins down, w_i; or to have different spins, b_i; where $i = 1, 2$ refers to nearest-neighbor pairs of sites along the field and perpendicular to it. Among these eight variables only three are independent, since they have to satisfy the normalization conditions

$$x + y = 1, \qquad z_i + 2b_i + w_i = 1, \qquad i = 1, 2 \tag{3.17}$$

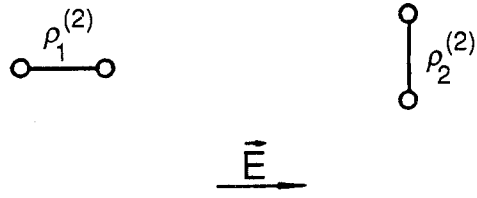

Fig. 1. In the presence of a driving field E the pair probabilities along the field, $\rho_1^{(2)}$, and perpendicular to it, $\rho_2^{(2)}$, are no longer equal.

and the consistency relations

$$\left.\begin{aligned} z_i &= b_i + x \\ w_i &= b_i + y \end{aligned}\right\}, \qquad i = 1, 2 \tag{3.18}$$

For example, one can choose as independent variables x, b_1, and b_2 and express the rest in terms of these. Instead of working with x, one can introduce the average magnetization per site $m = x - y$, which is the natural order parameter for the system. Since the system we are considering is diffusive, the local order parameter m is conserved under pair exchanges, and therefore its time evolution does not contribute a nontrivial algebraic equation at NESS. Nontrivial equations of motion can be derived only for the pair probabilities b_1 and b_2. In a similar way at every level of the MF approximation, one has $n-1$ nontrivial algebraic equations at NESS for n independent MF variables, due to normalization conditions, consistency relations, and conservation of the local magnetization. In the high-temperature regime the spontaneous magnetization is zero (completely disordered phase). The system of equations is then closed and can be solved numerically. However, at low enough temperatures, $m \neq 0$ and the system of equations is incomplete. By using only the homogeneous rate equations, it is not possible to obtain information concerning the transition temperature $T_c(E)$ or the low-temperature properties of the system.

We proceed further with deriving the rate equations at the pair level of approximation. Since our model system evolves only through exchanges of spins between nearest-neighbor sites, the change in energy associated with such exchange [see (2.5)] depends only on the surroundings of the given pair. Therefore, for deriving the rate equations for b_1 and b_2 we need to consider only clusters consisting of a bond and all its nearest neighbors. Since every spin can attempt exchange in both directions, we have to consider contributions $G_i^{(1)}$ and $G_i^{(2)}$ from the two clusters depicted in Fig. 2. The same configurations appearing on both clusters will have different probabilities due to the anisotropy induced by the electric field,

$$\frac{db_i}{dt} = [G_i^{(1)}(m, b_1, b_2; T_R, E) + G_i^{(2)}(m, b_1, b_2; T_R, E)], \qquad i = 1, 2 \tag{3.19}$$

$$G_i^{(k)}(m, b_1, b_2; T_R, E) = \sum_{\alpha} \Delta b_i \phi(\Delta H_\alpha + \varepsilon_\alpha^{(k)} E) P_\alpha^{(k)}, \qquad k = 1, 2 \tag{3.20}$$

The summation is over all configurations appearing on the clusters and $P_\alpha^{(k)}$ is the probability of a configuration α to occur on the cluster k from Fig. 2, and $\varepsilon_\alpha^{(k)}$ takes values $+1$, -1, or 0, depending on whether the exchange is along the field, against it, or perpendicular to it, respectively.

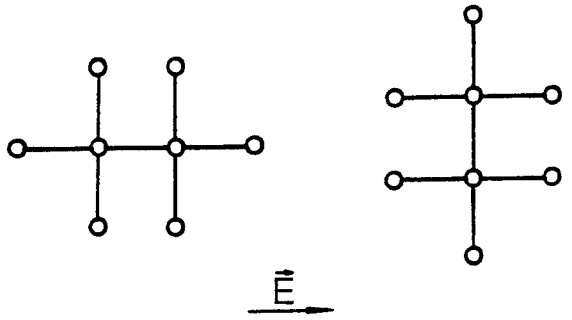

Fig. 2. On the pair level of approximation these are the smallest possible clusters that one has to consider in order to derive the rate equations for the fractions of $(+-)$ pairs along the field, b_1, and perpendicular to it, b_2.

To illustrate the derivation, let us consider a particular configuration appearing on the first cluster (Fig. 3) and calculate explicitly its contribution to the equations of motion (3.19). The probability of its occurring is given by

$$P_{\alpha}^{(1)} = \frac{z_1 b_1 w_1 z_2^2 b_2^2}{x^3 y^3} \tag{3.21}$$

and $\Delta H = 4J$, $\Delta b_1 = 2$, $\Delta b_2 = 0$, $\Delta m = 0$; thus its contributions to $G_1^{(1)}$ and $G_2^{(1)}$ are

$$2\phi(4J-E)\frac{z_1 b_1 w_1 z_2^2 b_2^2}{x^3 y^3} \quad \text{and} \quad 0 \tag{3.22}$$

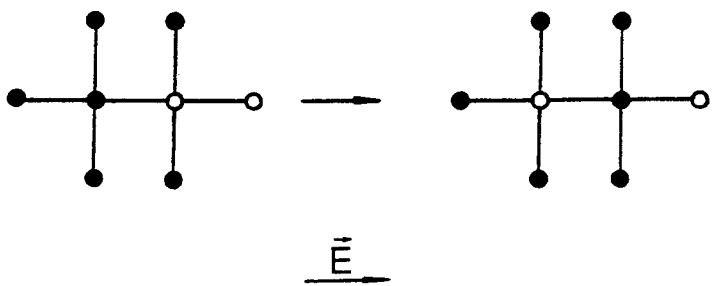

Fig. 3. An example of a particular configuration, illustrating the derivation of the rate equations. The black circles represent $(+)$ spins and the empty circles $(-)$ spins.

respectively. The contributions of the equivalent configuration of spins in the rotated cluster can be obtained from these by a simple interchange of the indices. The full expressions for $G_i^{(1)}$ and $G_i^{(2)}$ are very long and cumbersome and are given in the Appendix.

4. A MAXIMUM ENTROPY APPROACH

We conclude from the discussion above that the MF evolution equations (3.7)–(3.8) do not contain enough information to determine the probability distribution for the DDS in the phase-coexisting NESS regime. Here we attempt to overcome this problem by adopting a generalization of the Gibbsian approach due to Jaynes.[6–8] According to him, statistical mechanics (of nonequilibrium, as well as equilibrium systems) can be reduced to the general problem of Bayesian statistical inference. This approach leads to the determination of a probability distribution which corresponds to an optimal description of the system that is consistent with prior information about the physical laws governing the system. For example, this could be the knowledge of the equations of motion, conservation laws, moments of the probability distribution, etc. This prior knowledge is also reflected in the choice of the set of all accessible configurations on which the probability distribution is defined. In the absence of any further prior information about the system, it is assumed that the choice of the probability distribution should be as unbiased as possible. Mathematically, it is expressed through the maximum entropy principle (MEP): the optimal probability distribution $\rho(\{\sigma\})$ should maximize the information entropy functional, which is a measure of the missing information about the system. Any prior knowledge about the system can be accounted for by appropriate constraints on this variational principle. In particular, the normalization condition for the probability distribution is always imposed as such a constraint.

For our system, the entropy functional is defined as

$$S[\rho(\{\sigma\})] = -k_B \sum_{\{\sigma\}} \rho(\{\sigma\}) \log \rho(\{\sigma\}) \tag{4.1}$$

and the normalization constraint is

$$\sum_{\{\sigma\}} \rho(\{\sigma\}) = 1 \tag{4.2}$$

If a system achieves thermal equilibrium with a heat reservoir at a temperature T_R, the latter imposes an additional constraint of a fixed mean internal energy

$$\sum_{\{\sigma\}} H(\{\sigma\})\, \rho(\{\sigma\}) = U \tag{4.3}$$

The application of the MEP in this case leads to the usual canonical ensemble. It is well known that such an ensemble can be equivalently derived by minimizing the Helmholtz free energy

$$F[\rho(\{\sigma\})] = \sum_{\{\sigma\}} H(\{\sigma\})\,\rho(\{\sigma\}) - T_R S[\rho(\{\sigma\})] \tag{4.4}$$

which is a Legendre transform of the entropy functional. Note that for a system *at thermal equilibrium* with a heat reservoir at a temperature T_R, the thermodynamic temperature T of the system is by definition identical to T_R, where

$$T = \frac{\partial U}{\partial S} \tag{4.5}$$

Similarly, other ensembles of equilibrium statistical mechanics are recovered by imposing constraints on the maximization of the entropy arising from contacts with different types of reservoirs. In these cases as well, maximization of the entropy can be equivalently replaced by minimization of the corresponding thermodynamic potentials that are the appropriate Legendre transforms of the entropy. Thus, the MEP provides a unified approach to equilibrium statistical mechanics (see, e.g., refs. 9 and 10). Note that, as long as it is known that the system achieves thermodynamic equilibrium with the reservoirs, the determination of the corresponding probability distributions is independent of the particular way the contact with the appropriate reservoirs is realized. The reservoirs merely constrain the mean values of certain fluctuating system variables.

For $E = 0$, the system under consideration here can be considered at a thermal equilibrium with a heat reservoir at a temperature T_R that enters explicitly in the transition rates used in the Monte Carlo simulations. The choice of a particular form of the transition rates amounts to specifying an explicit energy exchange channel with the thermal reservoir. In addition, the choice of the transition rates uniquely specifies the stochastic evolution equation for the probability distribuition, and hence the stochastic equations of motion for its various moments. However, the theory of Markov chains shows that the *equilibrium* probability distribution is independent of the choice of the transition rates as long as they satisfy the condition of global detailed balance. Hence, at equilibrium, the various evolution equations resulting from different choices of the transition rates coincide, and lead to the same probability distribution as determined by the MEP.

For $E = 0$, the transition rates for the stochastic channel of energy exchange between the spin system and the heat reservoir at temperature T_R

are isotropic. In this case, the condition of global detailed balance is satisfied, and the system reaches equilibrium with the heat reservoir. The only effect of E in DDS is an additive contribution to energies entering in the stochastic rates that originates from work done by the electric field when a pair of spins are exchanged. We interpret it as a "field drive" (considered to be a part of the heat reservoir), which activates another, anisotropic, stochastic channel for energy exchange with the reservoir. As the condition of global detailed balance is violated for $E \neq 0$, the system cannot achieve equilibrium with the reservoir. Monte Carlo simulations show that in this case the system reaches a nonequilibrium steady state that is characterized by an inherent anisotropy and a stationary current. The energy of the spin system fluctuates in time due to energy exchanges with the heat reservoir, but its mean is stationary. The total energy of the combined system (spins and reservoir, including the stochastic field drive) is kept constant at any time. However, because of the anisotropy of the transition rates and the periodic boundary conditions, a stationary mean current is induced. We interpret the constant mean energy to arise from a steady rate of gain from the stochastic field drive, balanced by the same steady rate of loss to the rest of the reservoir. Since the condition of global detailed balance is not satisfied at NESS, the different choices of the transition rates lead to different stochastic equations of motion for the probability density and its moments at the steady state. Thus, at NESS, we expect the equations of motion to contain nonredundant prior information, which has to be incorporated as additional constraints for the variational determination of the steady-state probability distribution from MEP.

Other systems at NESS in thermal contact with a heat reservoir at temperature T_R have been previously studied using MEP by several authors.[31–33] It has been shown that, similarly to the equilibrium case, maximization of the entropy subject to the constraints of constant mean energy is again equivalent to minimization of a *generalized* Helmholtz free nergy having the same form as (4.4). It must be stressed, however, that the thermodynamic temperature (4.5) of the NESS system is in general not equal to T_R, and a steady heat flow may exist between the system and the heat reservoir. The minimization of the generalized Helmholtz free energy should be subject to additional constraints on the probability distribution expressing any other nonredundant prior information about the system. The DDS stochastic evolution equations for the probability distribution provide such constraints at NESS (those constraints become redundant at equilibrium).

The rest of this section is devoted to the application of MEP to DDS on the same level of MF approximation as we used for the derivation of the stochastic equations of motion in Section 3.

Consider the exact and most general expression for the generalized Helmholtz free energy, which is given by the minimum value of

$$\Psi = \sum_{\sigma_1} \cdots \sum_{\sigma_N} \rho^{(N)}(\sigma_1,\ldots,\sigma_N) \times H(\sigma_1,\ldots,\sigma_N) + k_B T_R \sum_{\sigma_1} \cdots \sum_{\sigma_N} \rho^{(N)}(\sigma_1,\ldots,\sigma_N) \times \ln \rho^{(N)}(\sigma_1,\ldots,\sigma_N) \tag{4.6}$$

considered as a functional of the joint probability distribution $\rho = \rho^{(N)}(\sigma_1,\ldots,\sigma_N)$ for the entire lattice, subject to the normalization condition constraint

$$\sum_{\sigma_1} \cdots \sum_{\sigma_N} \rho^{(N)}(\sigma_1,\ldots,\sigma_N) = 1 \tag{4.7}$$

Following Morita, we define the two following types of functionals of the reduced probability distributions. These are the functions $S^{(n)}$ defined via ln S which serve naturally as the entropy for the cluster $i_l,\ldots, i_n$,

$$\ln S^{(n)}(i_1,\ldots, i_n) = -\sum_{\sigma_{i_1}} \cdots \sum_{\sigma_{i_n}} \rho^{(n)}(\sigma_{i_1},\ldots, \sigma_{i_n}) \ln \rho^{(n)}(\sigma_{i_1},\ldots,\sigma_{i_n}) \tag{4.8}$$

In a way analogous to the way in which the correlation functions were defined, we now define the correlation functionals $F^{(n)}$:

$$F^{(2)}(i, j) = \frac{S^{(2)}(i, j)}{S^{(1)}(i)\, S^{(1)}(j)} \tag{4.9}$$

$$\vdots$$

$$F^{(n)}(i_1,\ldots, i_n) = \frac{S^{(n)}(i_1,\ldots, i_n)}{\left[\prod_{l=1}^{n} S^{(n)}(i_l) \prod_{\{l_1, l_2\}} F^{(2)}(i_{l_1}, i_{l_2}) \cdots \prod_{\{l_1,\ldots,l_{n-1}\}} F^{(n-1)}(i_{l_1},\ldots, i_{l_{n-1}})\right]} \tag{4.10}$$

In terms of $\rho^{(n)}$, $S^{(n)}$, and $F^{(n)}$ the following expression is found for the free energy, which is still exact:

$$\Psi = \sum_{\langle ij \rangle} \rho^{(2)}(\sigma_i, \sigma_j)\, H(\sigma_i, \sigma_j) - k_B T_R \left[\sum_{i=1}^{N} \ln S^{(n)}(i) + \sum_{\{i,j\}} F^{(2)}(i, j) + \sum_{\{i,j,k\}} F^{(3)}(i, j, k) + \cdots + \ln F^{(N)}(1,\ldots, N)\right] \tag{4.11}$$

Here we have used the fact that only nearest-neighbor interactions are included in the Hamiltonian (2.1). The minimum value of this expression cannot be found unless some approximations are made. As is shown by Morita, the various levels of approximation to the free energy in the framework of the CVM correspond to different choices of families of indecomposable small clusters. This is implemented by requiring (3.5) and also

$$F^{(k)}(i_1,\ldots,i_k)=1 \tag{4.12}$$

for all k point clusters that do not belong to some family of indecomposable clusters. Thus, on the pair level of approximation, in addition to (3.9)–(3.10) one also has

$$F^{(k)}(i_1,\ldots,i_k)=1 \qquad \text{for} \quad k>2 \tag{4.13}$$

$$F^{(2)}(i,j)=1 \qquad \text{for} \quad |i-j|>1 \tag{4.14}$$

Substituting (3.9)–(3.10) and (4.13)–(4.14) in (4.11) yields the following approximate expression for the free energy:

$$\begin{aligned}\Psi = &-J\sum_{i=1}^{N}\left[\rho^{(2)}(i,i+\hat{e}_1)+\rho^{(2)}(i,i+\hat{e}_2)\right]\\ &-k_{\mathrm{B}}T_R\left\{3\sum_{i=1}^{N}\ln S^{(1)}(i)+\sum_{i=1}^{N}\left[\ln S^{(2)}(i,i+\hat{e}_1)+\ln S^{(2)}(i,i+\hat{e}_2)\right]\right\}\end{aligned} \tag{4.15}$$

At this point, constrained minimization of (4.15) is still quite intractable. The homogeneity assumption (3.11)–(3.12), combined with the approximations made above, simplifies enormously the minimization procedure and makes the problem solvable. Using the notation introduced in Section 3, we obtain the following very simple expression for the free energy of an Ising ferromagnet in the presence of an electric field along one of the principal axes (e_1) at the pair level of approximation:

$$\Psi = N\psi$$

where

$$\begin{aligned}\psi = &J[(4b_1-1)+(4b_2-1)]\\ &-k_{\mathrm{B}}T_R\left[3(x\ln x+y\ln y)-\sum_{i=1}^{2}(z_i\ln z_i+2b_i\ln b_i+w_i\ln w_i)\right]\\ \equiv &\, u-T_R s\end{aligned} \tag{4.16}$$

We end this section with a short summary. Application of the MEP at the pair level of the homogeneous MF approximation reduces to the following mathematical problem. We have to minimize the expression (4.16) for the free energy with respect to the three independent MF variables b_1, b_2, and m describing the system, with the equations of motion for b_1 and b_2, (3.19), at NESS serving as constraints.

5. APPLICATION OF THE METHOD ON THE PAIR LEVEL OF APPROXIMATION

The minimization procedure outlined in the previous section was carried out numerically. One can find the constrained minimum in several ways. We have chosen to take the constraints explicitly. Thus, at fixed values of the parameters T_R and E, we solve the rate equations (3.19), with zero on the left-hand sides, numerically for b_1 and b_2 for every given value of the magnetization per site m. Upon substitution in the expression for the generalized free energy (4.16) one gets the latter only as a function of m, i.e.,

$$\psi = \psi(m, b_1(m; T_R, E), b_2(m; T_R, E); T_R, E) \tag{5.1}$$

This way, one has to minimize ψ with respect to only one variational parameter m. The results for the various physical quantities of interest are presented in this section, with all the energies given in units of J and the temperatures in units of k_B/J.

We first explored the dependence of the generalized free energy on the magnetization per site m. Thus, $\psi(m)$ was calculated and plotted considering T_R, the temperature of the reservoir, and E, the magnitude of the driving field, as parameters. These calculations indicate that a field-dependent critical temperature $T_c(E)$ can be defined. At reservoir temperatures $T_R \geqslant T_c(E)$, $\psi(m)$ is a convex function and has a single minimum at $m = 0$. This is usually interpreted as the existence of a single disordered phase in this regime. For $T_R < T_c(E)$, $\psi(m)$ has the familiar double-hump shape with two degenerate minima at $m_{1,2} = \pm\bar{m}$ and a maximum at $m_0 = 0$. Using a Maxwell construction, this can be interpreted as the occurrence of spontaneous symmetry breaking and the coexistence of two ordered phases at lower temperatures, similarly to the equilibrium case. Thus m emerges as a natural order parameter of the phase transition. Figure 4 displays $\psi(m)$ for $E \to \infty$ at three different temperatures. This behavior is typical for all values of the driving field strength.

The pair-level MEMF calculations indicate the existence of a second-order phase transition for all values of $0 \leqslant E < \infty$, in agreement with the Monte Carlo simulations. Figure 5 exhibits the dependence of m on T_R at

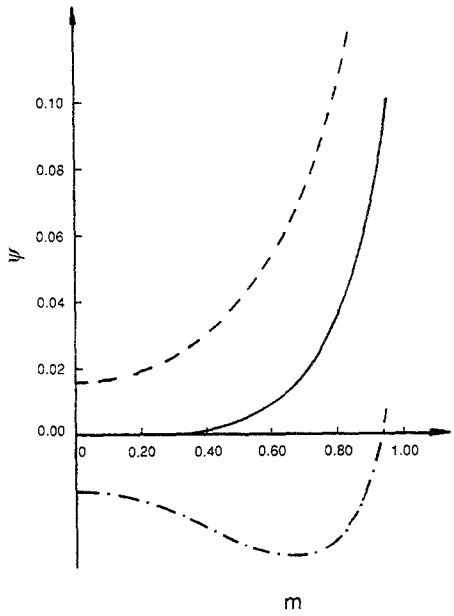

Fig. 4. The dependence of the free energy per site ψ on the order parameter m, for $E \to \infty$ at three different temperatures: $T_R > T_c(E \to \infty)$ (the dashed line); $T_R = T_c(E \to \infty)$ (the solid line); $T_R < T_c(E \to \infty)$ (the dash-dotted line).

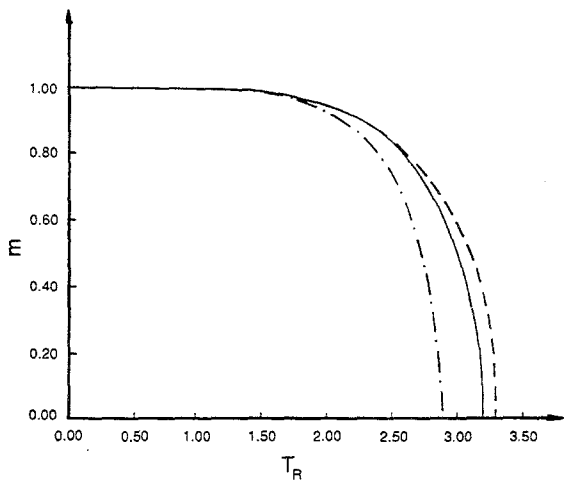

Fig. 5. The spontaneous magnetization m as a function of the temperature of the reservoir T_R at $E = 0$ (the dash-dotted line), $E = 10$ (the solid line), and $E \to \infty$ (the dashed line).

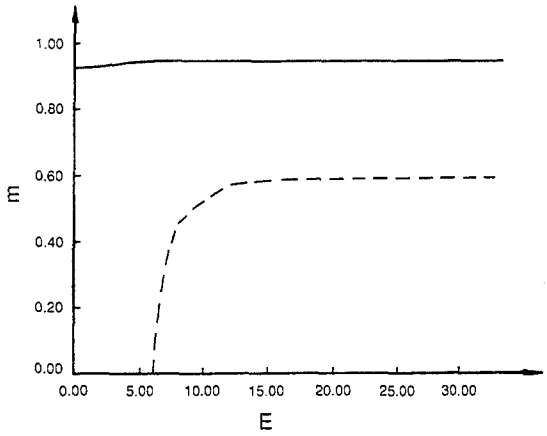

Fig. 6. The dependence of the order parameter on the strength of the electric field at $T_R = 3$ $[T_c(0) < T_R < T_c(\infty)]$ (the dashed line) and $T_R = 2$ $[T_R < T_c(0)]$ (the solid line).

equilibrium ($E = 0$), at $E = 10$, and in the infinite-field limit, indicating that the electric field induces a higher level of order. Figure 6 shows the variation of m with E at two fixed values of T_R below and above $T_c(0)$. Due to the nature of the Metropolis rate functions there are discontinuities in the slope of the curve at $E = 4, 8, 12$, as demonstrated in the inset of Fig. 7. This is an artifact of this particular choice of the transition rates and should not be attributed any physical significance.

The T_c–E phase diagram is presented in Fig. 8. The critical temperature increases monotonically with E, practically saturating for $E > 15$

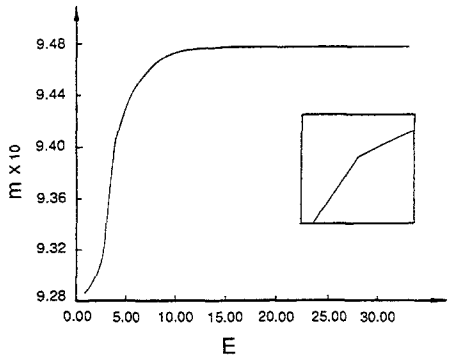

Fig. 7. The plot of the order parameter m versus the strength of the electric field E at $T_R = 2$ on a larger scale so that details can be seen. The inset is a further enlargement showing the discontinuity in the slope of $m(E)$ at $E = 4$. Similar discontinuities exist at $E = 8$ and 12 due to the singularities in the Metropolis rates.

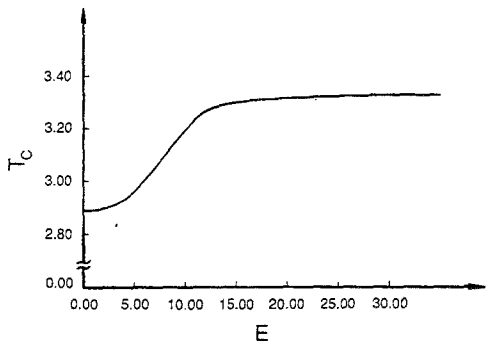

Fig. 8. The phase diagram for the ferromagnetic DDS in the T_R–E plane, calculated with Metropolis rates.

(at such high fields jumps against the field are almost totally suppressed). Our calculation for the equilibrium case yields $T_c(0) = 2.885$, which is the well-known result of Bethe's mean field approximation. In the limit of an infinitely strong field, the critical temperature reaches the saturation value of $T_c(E \to \infty) \approx 3.3228$ (for Metropolis rates). Thus, an infinitely strong field produces an increase of $\approx 15\%$ over the equilibrium critical temperature. On the same level of approximation the dynamic mean field theory of Dickman[11] estimates $T_c(E \to \infty) \approx 3.206$ (11% increase). All of these approximations are consistent with Monte Carlo data. Early results show $T_c(E \to \infty) = 3.125$[1,2] and 3.075.[15,18,19] The most recent estimate,[20] using anisotropic finite-size scaling, is 3.20, which is a 41% increase over the exact $T_c(0) = 2.269$.

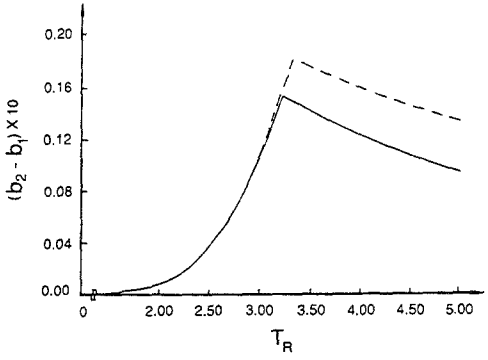

Fig. 9. The difference between the fraction of $(+-)$ nearest-neighbor pairs in the direction perpendicular to the field b_2, and along the field, b_1, versus the temperature T_R at $E = 10$ (the solid line) and $E \to \infty$ (the dashed line).

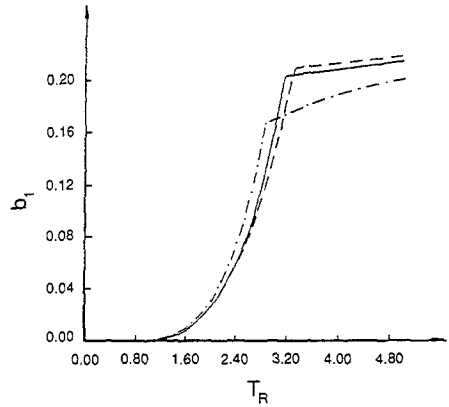

Fig. 10. The nearest-neighbor pair probability of having $(+-)$ spins in direction of the field, b_1, as a function of T_R at equilibrium ($E=0$) (the dash-dotted line), $E \approx 10$ (the solid line), and $E \to \infty$ (the dashed line); b_2 has a similar behavior.

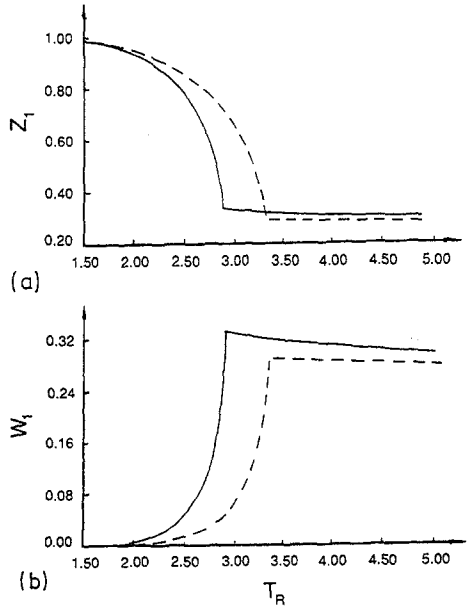

Fig. 11. The temperature dependence of the nearest-neighbor pair probabilities along the field (a) for having $(++)$ spins, z_1, and (b) for having $(--)$ spins, w_1. The solid line presents the results at $E=0$ and the dashed at $E \to \infty$.

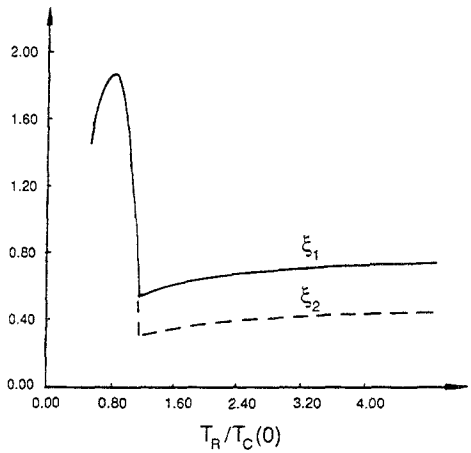

Fig. 12. The nearest-neighbor pair correlations along the field, ξ_1, and perpendicular to it, ξ_2 (multiplied by T_R) versus the reduced temperature $T_R/T_c(0)$ at $E \to \infty$.

Figures 9–13 display how the nearest-neighbor pair probabilities b_i, z_i, and w_i, $i = 1, 2$, are affected by the presence of a driving field. As expected, the field induces certain anisotropy and the probabilities in directions parallel and transverse to the field are no longer equal, though their values are still quite close. The difference between fractions of up–down spin pairs, $b_2 - b_1$, versus the temperature T_R is plotted in Fig. 9. The maximum is attained at $T_c(E)$. As $T_R \to 0$ both b_1 and b_2 approach zero (see also

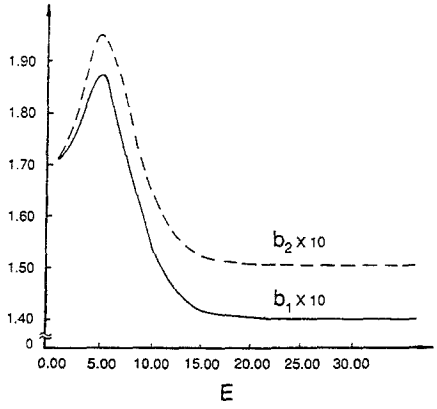

Fig. 13. The nearest-neighbor pair probabilities of having $(+-)$ spins along the field, b_1 (the solid line), and perpendicular to it, b_2 (the dashed line), versus the electric field E at $T_R = 3$ $[T_c(0) < T_R < T_c(\infty)]$.

Fig. 10), which corresponds to a completely ordered state. The corresponding behavior of the nearest-neighbor fractions along the field of up–up (z_1) and down–down spins (w_1) is presented in Fig. 11. In the limit of $T_R \to \infty$, at finite fields, b_1 and b_2 are expected to approach 1/4 (correspondingly, $b_2 - b_1 \to 0$). The number of broken bonds (in both directions) in the ordered phase raises rapidly with T_R until the transition temperature is reached. In the disordered phase the growth rate toward the saturation value is much slower. This qualitative behavior is the same for $E=0$ and $E \neq 0$. For $T_R < T_c(0)$ the electric field is responsible for a higher level of ordering in the system since $b_i(E) < b(0)$. In the high-temperature regime, however, the field stimulates a higher level of disorder, the effect being more pronounced in transverse direction, as could also be seen from Fig. 12, where the nearest-neighbor pair correlations ξ_1 and ξ_2 are defined by $\xi_k = \langle \sigma(i)\, \sigma(i+\hat{e}_1) \rangle$, $k = 1, 2$. The behavior of b_1 and b_2 depicted in Fig. 13 can be easily understood if compared with Figs. 6 and 8. At $T_R = 3$ the system is initially in the disordered phase. The application of the electric field at first increases the level of disorder until a maximum is achieved at $E \approx 5$. Then the tendency of the ordering starts prevailing and for $E \geqslant 6.5$ the system is in the ordered phase with b_1 and b_2 decreasing rapidly toward the saturation values, which are lower than the equilibrium value at that temperature. The entropy per site (Fig. 14) has the same qualitative behavior as b_1 and b_2 (see also Fig. 22a).

Another quantity of interest, which is readily computed in our theory, is the average current in the direction of the field $\mathbf{J} = j\hat{e}_1$. The current for the bond $(i, i+\hat{e}_1)$ is defined by

$$\mathbf{J}(i; \{\sigma\}) = \phi_E(i, i+\hat{e}_1, \{\sigma\})(\sigma_i - \sigma_{i+\hat{e}_1})/2 \tag{5.2}$$

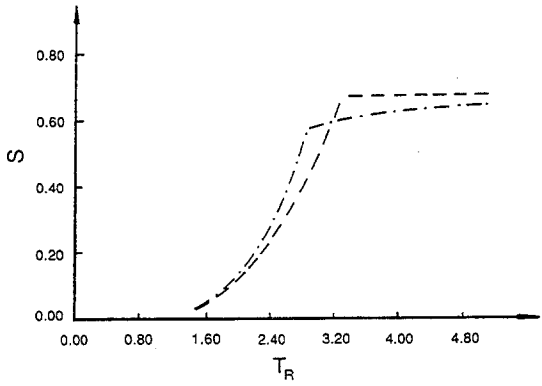

Fig. 14. The entropy per site s versus the temperature of the reservoir T_R at $E=0$ (the dashed-dotted line) and $E \to \infty$ (the dashed line).

i.e., this is the expected jump rate from i to $i+\hat{e}_1$ in a configuration $\{\sigma\}$ (by the homogeneity assumption it is the same for all i). By averaging over all possible configurations appearing on a cluster consisting of a bond and all its nearest neighbors (cluster 1, introduced in Section 3), one gets the average current at a pair level of approximation. It could be written in the form

$$j = n_+ - n_- \tag{5.3}$$

with

$$n_\pm = \sum_\alpha \phi(\Delta H_\alpha \mp E) P_\alpha^{(1)} \tag{5.4}$$

n_+ and n_- are the average number of jumps performed along and opposite to the field, respectively. The full expression for the current j is given in the Appendix. At $T_R = 2$ $[T_R < T_c(0)]$, j first increases linearly with E and saturates rapidly after $E = 5$ (Fig. 15). At this temperature the system is always in the ordered phase and the current is strongly suppressed. At higher temperatures $[T_c(0) < T_R < T_c(E \to \infty)]$, j increases considerably for $E \in [0, 6.5]$, since for these values of E the system is in the disordered phase. At high temperatures and strong field $j \approx b_1$ (see Fig. 16). The temperature dependence of the current has a break in its slope at $T_c(E)$, consistent with the results from MC simulations.[1,2,18]

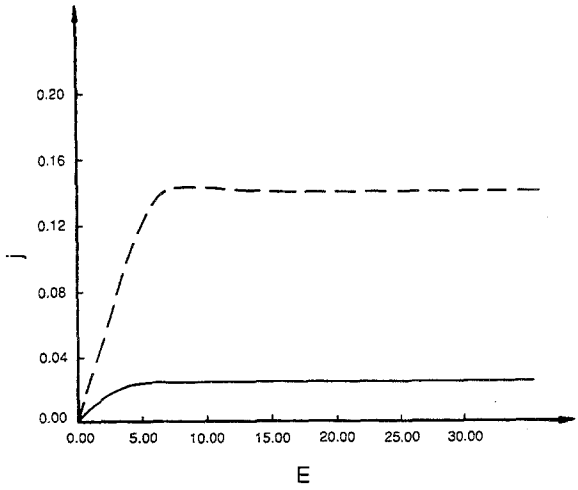

Fig. 15. The average electric current j in the steady state as a function of the electric field E at two different temperatures, $T_R < T_c(0)$ (the solid line) and $T_c(0) < T_R < T_c(\infty)$ (the dashed line).

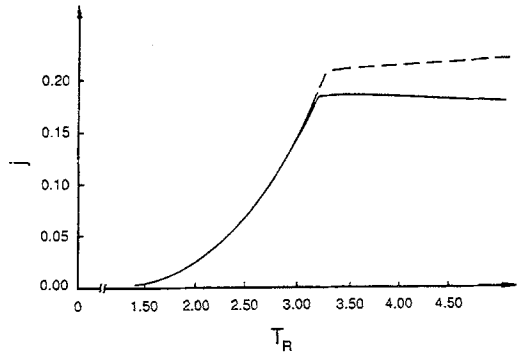

Fig. 16. The temperature dependence of the average electric current j in the direction of the field at two values of the driving field strength, $E = 10$ (the solid line) and $E \to \infty$ (the dashed line).

Since the system is not in equilibrium with the heat reservoir, it might be expected that it is characterized by some effective temperature different from that of the reservoir. If, in analogy with the equilibrium case, one defines a quantity

$$\tilde{T} = \frac{\partial u}{\partial s} \tag{5.5}$$

one can try to interpret it as the temperature of the system. In equilibrium this relation follows from the identification of the statistical entropy with

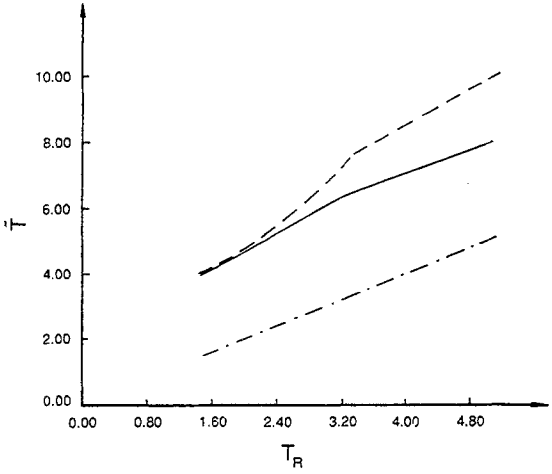

Fig. 17. The temperature dependence of the derivative of the internal energy ($\tilde{T} = \partial u/\partial s$) with respect to the entropy at fixed difference $b_2 - b_1$ in the steady state of the system at $E = 0$ (the dash-dotted line), $E = 10$ (the solid line), and $E \to \infty$ (the dashed line).

the thermodynamic entropy. For a system in the nonequilibrium state, however, there is no evidence so far that the same identification can be made. As can be seen from Fig. 17, $\tilde{T}(E) > T_R$ at $E > 0$ (at $E = 0$, $\tilde{T} = T_R$, of course). This result is consistent with the fact that there is a constant flow of heat from the system to the reservoir. Aside from this, there is no other evidence that T could indeed be viewed as the temperature of the system. The dependence of $\tilde{T}$ on E is shown in Fig. 18 and has the typical behavior displayed by the other physical quantities, i.e., it saturates as $E \to \infty$.

We studied also the efect of using different rates in the rate equations on the properties of DDS at NESS. As mentioned above, the choice of the rates is of no importance in equilibrium, but at NESS it is expected that the choice of transition rates might affect the properties of the system. The dependences of various quantities of interest as a function of the temperature T_R at fixed E and as a function of E at fixed T_R calculated with different rates are displayed in Figs. 18–22. The basic observations are: (i) for Kawasaki rates the results we get are very close to those obtained with the Metropolis rates. This is expected, since the Kawasaki rates are essentially smoothed versions of the Metropolis rates. For example, $T_c(E \to \infty)$ computed with the Kawasaki rates is ≈ 3.326, which is a negligible change over the result (3.3228) computed with the Metropolis rates;

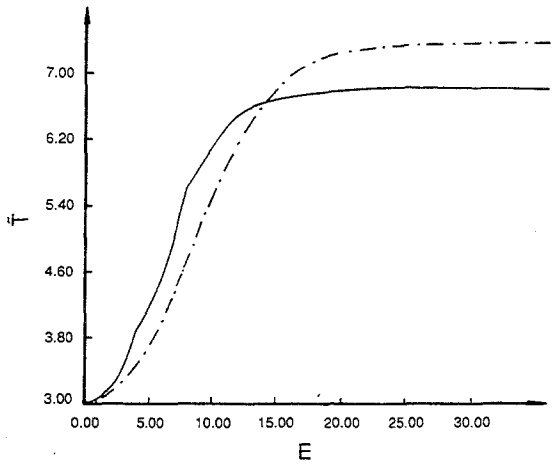

Fig. 18. The derivative of the internal energy u with respect to the entropy s, $\tilde{T}$ (for fixed difference $b_2 - b_1$), in the steady state as a function of the driving field strength E at $T_c(0) < T_R < T_c(\infty)$ for Metropolis rates (the solid line) and Kawasaki rates (the dash-dotted line).

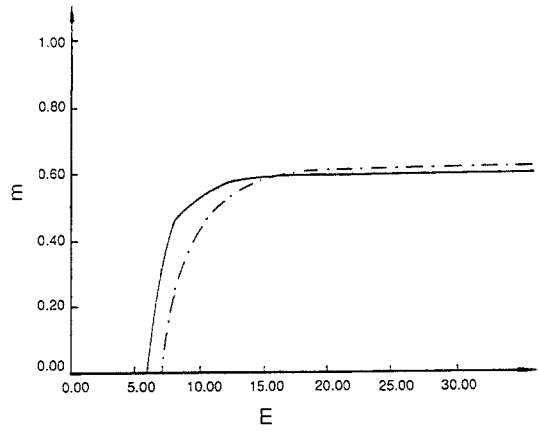

Fig. 19. The spontaneous magnetization m at $T_R = 3$ $[T_c(0) < T_R < T_c(\infty)]$ as a function of the strength of the driving field E computed with the Metropolis rates (the solid line) and the Kawasaki rates (the dash-doted line). In the case of van Beijeren–Schulman rates m is the same as in the equilibrium case at this temperature (i.e., it is zero).

(ii) on the other hand, the use of the van Beijeren–Schulman rates leads to a dramatic change. Except for the current, all other nonequilibrium steady-state quantities are the same as in equilibrium. This result can be traced back to the specific form of the van Beijeren–Schulman rates and the way the driving field enters into the dynamical equations for b_1 and b_2. In other

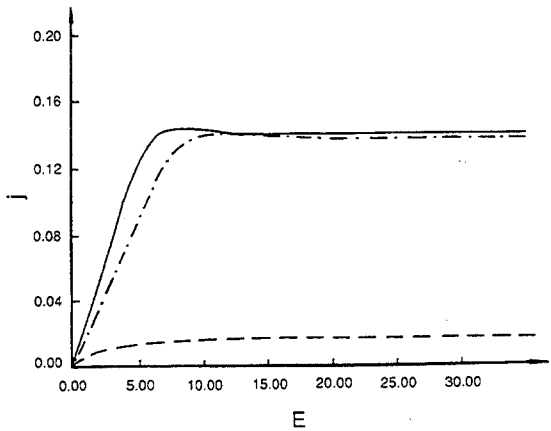

Fig. 20. The dependence of the average electric current per site j on the strength of the electric field E at $T_c(0) < T_R < T_c(\infty)$ in the case of Metropolis rates (the solid line), Kawasaki rates (the dash-dotted line), and van Beijeren–Schulman rates (the dashed line).

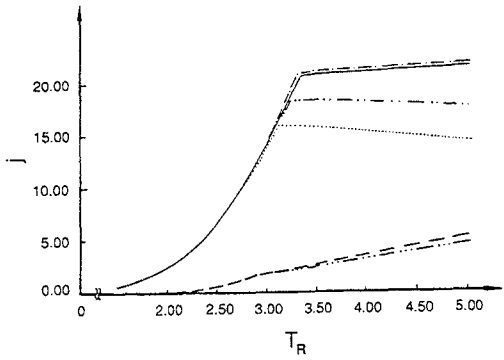

Fig. 21. For comparison the average electric current per site j is shown as a function of the temperature T_R at different values of the driving field and different rates on the same plot: (i) $E \to \infty$ (Metropolis rates, the solid line; Kawasaki rates, the dash-dotted line; and van Beijeren–Schulman rates, the dashed line; (ii) $E = 10$ (Metropolis rates; the dotted line; Kawasaki rates, the dash-two-dot line; van Beijeren–Schulman rates, the dash-three-dot line).

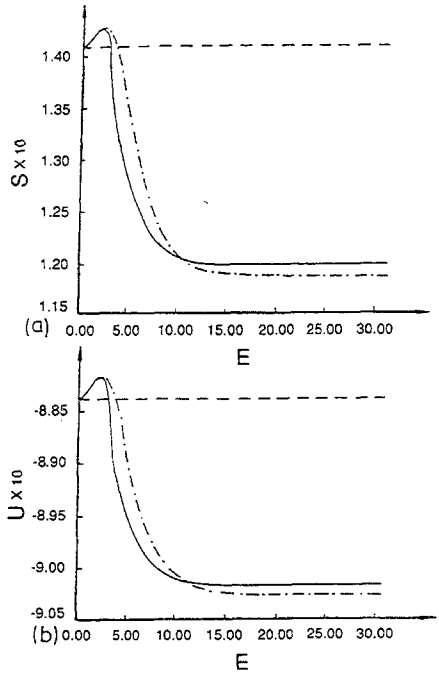

Fig. 22. (a) The entropy per site s and (b) the internal energy per site u of the system in the steady state as functions of the driving field strength E at $T_c(0) < T_R < T_c(\infty)$. The results are presented for Metropolis rates (the solid line), Kawasaki rates (the dash-dotted line), for van Beijeren–Schulman rates (the dashed line).

words, at the pair level of approximation, E enters through the same overall factor in both rate equations. Such a factor can be absorbed into a change of the time scale. It is not clear if this is an artifact of the pair level of approximation, or whether it persists at higher MF levels of approximation as well.

6. CONCLUSIONS

A rich variety of analytical methods exists for studying phase transitions in equilibrium systems, ranging from simple mean field approximations to renormalization group techniques. By contrast, the arsenal of available approximate methods is much scarcer for systems at NESS. This is partly due to the weaker foundations of nonequilibrium statistical mechanics as compared to the well-established Gibbsian ensemble approach for equilibrium systems. The latter serves as a natural basis for many approximations. Thus, it is not surprising that the initial studies of DDS and other systems at NESS centered around Monte Carlo simulations. These simulations provided a wealth of interesting and valuable information on nonequilibrium phase transitions. However, there is a need for a parallel development of approximate analytical methods applicable to such systems, not only as computational alternatives, but as a means for guiding the simulations, deriving basic principles, and organizing our knowledge. Thus, in the case of DDS, there has been an ongoing effort to extend approximation approaches, such as field-theoretic renormalization group and lattice-gas mean field methods, from equilibrium to NESS. In this paper we have investigated the DDS model, which is a particularly simple system at NESS exhibiting a phase transition, by using the maximum entropy principle. The Kolmogorov–Shannon entropy functional for the NESS probability distribution over the possible configurations of the Ising variables is constructed in the usual way. The DDS is assumed to be in thermal contact with a heat reservoir at a constant temperature T_R. As has been previously shown, maximization of the entropy in this case is equivalent to minimization of a generalized Helmholtz free energy. In Section 4 we argued the applicability of this result for the DDS. For nonvanishing applied electric field, the DDS is driven into NESS by its stochastic equations of motion. Thus we have used the latter as additional *constraints* to be imposed on the minimization of the generalized Helmholtz free energy.

Based on the assumptions above, we have developed a systematic mean field approximation method which is an extension of the Kikuchi cluster variation method for lattice models at equilibrium. Here, the

method has been demonstrated for the DDS on the square lattice using the homogeneous pair level of approximation. This approximation was applied to both the stochastic equations of motion and to the generalized Helmholtz free energy. It has been shown that the homogeneous MF approximation to the evolution equations does not provide a closed self-consistent system of equations for the variational parameters, except for the disordered phase. However, using these equations as additional constraints for the generalized Helmholtz free energy and with the help of a Maxwell construction, we were able to derive a MF phase diagram that is a good approximation to the phase diagram derived from Monte Carlo simulations. Moreover, we were able to study and predict properties of the DDS that cannot be easily addressed by Monte Carlo simulation methods, such as the behavior of the entropy-related properties. Our study recovers all the basic bulk properties of the system as reported from Monte Carlo simulations to the extent that can be expected from a mean field treatment. On the other hand, our attempts to base a similar kind of MF approximation on other variational principles did not lead to MF phase diagrams even remotely comparable to the one observed in simulations.

Among the variational principles sometimes advocated for non-equilibrium systems, we have explicitly checked the minimum entropy production principle and the possibility of using the constraint of constant electric current in conjunction with the MEP. This has been done on the same homogeneous pair level of the MF approximation as we have done above using the MF evolution equations as the constraints. Within this level of the MF approximation, explicit expressions for the current and the entropy production can be easily derived. However, we find that using either the minimum entropy production principle or imposing the constraint of constant electric current in conjunction with the MEP does not reproduce the Monte Carlo results even qualitatively (there is no phase separation at all at any value of the electric field).

Quite generally, for systems whose time evolution can be modeled by a Markov chain, the probability distribution is given by the solution of the linear master equation. If the system is in a thermal equilibrium with a heat reservoir, it satisfies global detailed balance. In that case, the long-time limit of the solution to the master equation minimizes the Helmholtz free energy, and it is independent of the particular form of the channel for the thermal contact. Thus, at equilibrium, the evolution equations contain redundant information with respect to that obtained from minimization of the Helmholtz free energy. However, at NESS, the global detailed balance is not satisfied. In principle, one can resort to solving the exact linear master equation for the evolution probability distribution. For most physical systems such an exact solution is impossible to find. However,

approaching NESS in the spirit of MEP, one should view the evolution equations as additional constraints to be imposed on the minimization of the generalized Helmholtz free energy. These evolution equations depend now on the specific form of the thermal channel between the system and the heat reservoir. Mean field approximations similar to those used for equilibrium systems can then be employed to find approximate solutions to the constrained minimization problem. This work demonstrates the usefulness of such an approach for generating a hierarchy of mean field approximations for the DDS. We limited the scope of our numerical study to the pair level of MF approximation for the ferromagnetic DDS on the square lattice. However, the accuracy of this method can be systematically improved by going to larger cluster approximations. Using the coherent anomaly method due to Suzuki,[34,35] scaling between MF results from different levels of approximation can provide accurate information about critical behavior and serve as a basis for an alternative RG approach to DDS. Furthermore, relaxation of the lattice translational invariance assumption may adapt the MF approximation suggested here for studying wetting and interfacial phenomena in DDS.

In this work we have concentrated on the application of the maximum entropy mean field method to the DDS. This is a particularly simple system, for which many simulation results are available. Thus, it provides a useful test of the basic principles behind the MEMF method. However, we believe that this approach is quite general, and can be extended to other systems for which the equation of motion is known, in stochastic, hydrodynamic, or possibly even deterministic forms.

APPENDIX

$$
\begin{aligned}
G_1^{(1)} = \frac{b_1}{x^3 y^3} \{ & [\phi(12-E)+\phi(12+E)]\, z_1 w_1 z_2^2 w_2^2 \\
& - [\phi(-12-E)+\phi(-12+E)]\, b_1^2 b_2^4 \\
& + 2[\phi(8-E)+\phi(8+E)]\, z_1 w_1 z_2 w_2 (z_2+w_2) b_2 \\
& - 2[\phi(-8+E)+\phi(-8+E)]\, b_1^2 b_2^2 (z_2+w_2) b_2 \\
& + [\phi(4-E)+\phi(4+E)]\{ z_1 w_1 b_2^2 [(z_2+w_2)^2 + 2 z_2 w_2] - b_1^2 z_2^2 w_2^2 \} \\
& - [\phi(-4-E)+\phi(-4+E)]\, b_2^2 \{ b_1^2 [(z_2+w_2)^2 + 2 z_2 w_2] - z_1 w_1 b_2^2 \} \\
& + 2[\phi(-E)+\phi(E)](-b_1^2 z_2 w_2 + z_1 w_1 b_2^2)(z_2+w_2) b_2 \}
\end{aligned}
$$

$$G_1^{(2)} = \frac{4b_2}{x^3y^3}\{\phi(12)\, z_1^2 w_1^2 z_2 w_2 - \phi(-12) b_1^4 b_2^2$$
$$+ \phi(8)[z_1 b_1 w_1 z_2 w_2 (z_2 + w_2) + z_1^2 w_1^2 b_2 (z_2 + w_2)]$$
$$- \phi(-8)[b_1^3 b_2^2 (z_2 + w_2) + b_1^4 b_2 (z_2 + w_2)]$$
$$+ \phi(4)[z_1 b_1 w_1 b_2 (z_1 + w_1)(z_2 + w_2) + z_1^2 w_1^2 b_2^2]$$
$$- \phi(-4)[b_1^3 b_2 (z_1 + w_1)(z_2 + w_2) + b_1^4 z_2 w_2]$$
$$+ [z_1 b_1 w_1 b_2^2 (z_2 + w_2) - b_1^3 z_2 w_2 (z_1 + w_1)]\}$$

$$G_2^{(1)} = \frac{2b_1}{x^3y^3}\{[\phi(12 - E) + \phi(12 + E)]\, z_1 w_1 z_2^2 w_2^2$$
$$- [\phi(-12 - E) + \phi(-12 + E)] b_1^2 b_2^4$$
$$+ [\phi(8 - E) + \phi(8 + E)]\, z_2 w_2 [z_1 w_1 b_2 (z_2 + w_2) + b_1 z_2 w_2 (z_1 + w_1)]$$
$$- [\phi(-8 - E) + \phi(-8 + E)]\, b_1^2 b_2^3 [b_1 (z_2 + w_2) + b_2 (z_1 + w_1)]$$
$$+ [\phi(4 - E) + \phi(4 + E)]\, b_1 z_2 w_2 [b_2 (z_1 + w_1)(z_2 + w_2) + b_1 z_2 w_2]$$
$$- [\phi(-4 - E) + \phi(-4 + E)]\, b_2^3 [b_1 (z_1 + w_1)(z_2 + w_2) + b_2 z_1 w_1]$$
$$+ [\phi(-E) + \phi(+E)]\, b_2 (z_2 + w_2)(b_1^2 z_2 w_2 - b_2^2 z_1 w_1)\}$$

$$G_2^{(2)} = \frac{2b_2}{x^3y^3}(\phi(12)\, z_1^2 w_1^2 z_2 w_2 - \phi(-12) b_1^4 b_2^2$$
$$+ \phi(8)\, 2b_1 z_1 w_1 z_2 w_2 (z_1 + w_1) - \phi(-8)\, 2b_1^3 b_2^2 (z_1 + w_1)$$
$$+ \phi(4)\{b_1^2 z_2 w_2 [(z_1 + w_1)^2 + 2z_1 w_1] - b_2^2 z_1^2 w_1^2\}$$
$$- \phi(-4)\, b_1^2 \{b_2^2 [(z_1 + w_1)^2 + 2z_1 w_1] - b_1^2 z_2 w_2\}$$
$$+ 2b_1 (z_1 + w_1)(-b_2^2 z_1 w_1 + b_1^2 z_2 w_2))$$

$$j = \frac{b_1}{x^3y^3}([\phi(12 - E) - \phi(12 + E)]\, z_1 w_1 z_2^2 w_2^2$$
$$+ [\phi(-12 - E) - \phi(-12 + E)]\, b_1^2 b_2^4$$
$$+ [\phi(8 - E) - \phi(8 + E)] z_2 w_2 [2z_1 w_1 b_2 (z_2 + w_2) + b_1 z_2 w_2 (z_1 + w_1)]$$
$$+ [\phi(-8 - E) - \phi(-8 + E)] b_1 b_2^3 [2b_1 (z_2 + w_2) + b_2 (z_1 + w_1)]$$
$$+ [\phi(4 - E) - \phi(4 + E)]\{2b_1 b_2 z_2 w_2 (z_1 + w_1)(z_2 + w_2)$$
$$+ b_2^2 z_1 w_1 [(z_2 + w_2)^2 + 2z_2 w_2] + b_1^2 z_2^2 w_2^2\}$$

$$+[\phi(-4-E)-\phi(-4+E)]\,b_2^2\{2b_1b_2(z_1+w_1)(z_2+w_2)$$
$$+b_1^2[(z_2+w_2)^2+2z_2w_2]+b_2^2z_1w_1\}$$
$$+[\phi(-E)-\phi(+E)]\,b_2[b_1b_2(z_1+w_1)(z_2+w_2)^2+2z_2w_2]$$
$$+2(z_2+w_2)(b_1^2z_2w_2+b_2^2z_2w_2+b_2^2z_1w_1))$$

ACKNOWLEDGMENTS

We thank J. L. Lebowitz, J. L. Valles, M. Q. Zhang, and R. Dickman for useful discussions. Most of this work was done while two of the authors (N.C.P. and Y.S.) were at Virginia Polytechnic Institute and State University. The hospitality of Profs. G. L. Jones at the University of Notre Dame and Y. Shapir at the University of Rochester, where parts of this work were completed, is gratefully acknowledged. N.C.P. would also like to thank Prof. P. F. Zweifel for support and encouragement, and Eastman Kodak Company for partial support. This research is supported in part by grants from the National Science Foundation through the Division of Materials Research.

REFERENCES

1. S. Katz, J. L. Lebowitz, and H. Spohn, *Phys. Rev. B* **28**:1655 (1983).
2. S. Katz, J. L. Lebowitz, and H. Spohn, *J. Stat. Phys.* **34**:497 (1984).
3. R. J. Glauber, *J. Math. Phys.* **4**:294 (1963).
4. K. Kawasaki, *Phys. Rev.* **145**:224 (1966).
5. K. Kawasaki, in *Phase Transitions and Critical Phenomena*, Vol. 2, C. Domb and M. S. Green, eds. (Academic Press, New York, 1972).
6. E. T. Jaynes, *Phys. Rev.* **106**:620 (1957).
7. E. T. Jaynes, *Phys. Rev.* **108**:171 (1957).
8. E. T. Jaynes, in *Papers on Probability, Statistics and Statistical Physics*, R. D. Rosenkrantz, ed. (Reidel, Dordrecht, 1983).
9. W. T. Grandy, Jr., *Foundations of Statistical Mechanics*, (Reidel, Dordrecht, 1987).
10. C. R. Smith and W. T. Grandy Jr., eds. *Maximum-Entropy and Bayesian Methods in Inverse Problems* (Reidel, Dordrecht, 1985).
11. R. Dickman, *Phys. Rev. A* **38**:2588 (1989).
12. R. G. Bowers and A. McKerrel, *Am. J. Phys.* **46**:138 (1978).
13. J. Krug, J. L. Lebowitz, H. Spohn, and M. Q. Zhang, *J. Stat. Phys.* **44**:535 (1986).
14. J. Marro, J. L. Lebowitz, H. Spohn, and M. H. Kalos, *J. Stat. Phys.* **38**:725 (1985).
15. J. L. Valles and J. Marro, *J. Stat. Phys.* **49**:89 (1987).
16. K. Leung and J. L. Cardy, *J. Stat. Phys.* **44**:567 (1986).
17. H. K. Janssen and B. Schmittmann, *Z. Phys. B* **64**:503 (1986).
18. J. L. Valles and J. Marro, *J. Stat. Phys.* **43**:441 (1986).
19. J. Marro, J. L. Valles, and J. M. Gonzales-Miranda, *Phys. Rev. B* **35**:3372 (1987).
20. K. T. Leung, *Phys. Rev. Lett.* **66**:453 (1991).
21. H. van Beijeren and L. S. Schulman, *Phys. Rev. Lett.* **53**:806 (1984).

22. R. Dickman, *Phys. Rev. A* **41**:2192 (1990).
23. P. L. Garrido, J. Marro, and R. Dickman, *Ann. Phys.* **199**:366 (1990).
24. B. Schmittmann, *Int. J. Mod. Phys. B* **4**:2269 (1990).
25. R. Kikuchi, *Phys. Rev.* **81**:988 (1951).
26. T. Morita, *J. Phys. Soc. Jpn.* **12**:753 (1957).
27. N. G. van Kampen, in *Advances in Chemical Physics*, Vol. 34, I. Prigogine and S. A. Rice, eds. (Wiley, New York, 1976), p. 245.
28. C. M. van Baal, *Physica A* **111**:591 (1982).
29. I. I. Kidin and M. A. Shtremel, *Fiz. Metal. Metalloved.* **11**:641 (1961).
30. N. Pesheva, Derivation of the macroscopic rate equations for DDS at pair level of approximation, to be published.
31. I. Procaccia and J. Ross, *J. Chem. Phys.* **67**:5558 (1977).
32. I. Procaccia, Y. Shimoni, and R. D. Levine, *J. Chem. Phys.* **65**:3284 (1976).
33. I. Procaccia and R. D. Levine, *J. Chem. Phys.* **65**:3357 (1976).
34. M. Suzuki, *J. Phys. Soc. Jpn.* **55**:4205 (1986).
35. M. Suzuki, M. Katori, and X. Hu, *J. Phys. Soc. Jpn.* **56**:3092 (1987).